9-1-1995

New Sources for the Hot Oxygen Geocorona: Solar Cycle, Seasonal, Latitudinal, and Diurnal Variations

Michael P. Hickey Ph.D.
Embry-Riddle Aeronautical University, hicke0b5@erau.edu

P. G. Richards
University of Alabama - Huntsville

D. G. Torr
University of Alabama - Huntsville

JOURNAL OF GEOPHYSICAL RESEARCH, VOL. 100, NO. A9, PAGES 17,377–17,388, SEPTEMBER 1, 1995

New sources for the hot oxygen geocorona: Solar cycle, seasonal, latitudinal, and diurnal variations

M. P. Hickey

Optical Aeronomy Laboratory and Center for Space Plasma and Aeronomic Research, University of Alabama in Huntsville

P. G. Richards

Computer Science Department and Center for Space Plasma and Aeronomic Research, University of Alabama in Huntsville

D. G. Torr

Physics Department and Center for Space Plasma and Aeronomic Research, University of Alabama in Huntsville

Abstract. This paper demonstrates the variability of thermospheric sources of hot oxygen atoms. Numerical calculations were performed for day and night, high and low solar activity, summer and winter, and low- and middle-latitude conditions. Under most conditions, reactions involving metastable species are more important hot O sources than previously considered dissociative recombination of O_2^+ and NO^+. All the hot O sources are an order of magnitude lower at midnight than at noon. At night, dissociative recombination of O_2^+ and NO^+ are the most important sources. Quenching of vibrationally excited N_2 (N_2^*) by O is the most important metastable source at night. Above 300 km, hot O sources increase by an order of magnitude between solar minimum and solar maximum. For a given level of solar activity, the high-altitude total production rate of hot O kinetic energy is greater during winter than during summer, indicating a dominance of cooler hot O sources during summer. The N_2^* source dominates at low altitudes. At high altitudes it is almost negligible at solar minimum, but increases to become the dominant source at solar maximum. Atomic oxygen quenching of $N(^2D)$ is a large source at solar minimum and is still important at solar maximum. Overall, seasonal variations are small compared to solar cycle, diurnal and latitudinal variations. While quenching of metastable species is more important at midlatitudes than at low latitudes, there is little latitudinal variation in hot O production due to dissociative recombination of NO^+ and O_2^+.

1. Introduction

The possibility of a hot oxygen geocorona was originally discussed by *Rohrbaugh and Nisbet* [1973]. They calculated the flux of energetic atoms resulting from the dissociative recombination of O_2^+ and NO^+ in the *F* region of the Earth's ionosphere, and found that the hot atoms can ascend to altitudes of several thousand kilometers and can travel horizontally to distances of the order of the Earth's radius.

Following the work of *Rohrbaugh and Nisbet* [1973], *Torr et al.* [1974] suggested that energetic oxygen atoms can also be produced by precipitating energetic O^+ ions during magnetically disturbed periods. Such energetic O^+ fluxes have been reported by *Shelley et al.* [1972]. *Torr et al.* [1974] investigated the angular and energy distributions of the energetic oxygen atoms. Later theoretical calculations were performed by *Yee and Hays* [1980] and *Ishimoto et al.* [1986, 1992].

The possibility of the existence of hot O coronas in other planetary atmospheres has also received attention. Theoretical studies of the hot O corona of Mars began with the suggestion of *McElroy* [1972] that the dissociative recombination of O_2^+ would produce fast O atoms with a kinetic energy of 2.5 eV. Later, hot O calculations were performed by *Knudsen* [1973], while more recently, *Ip* [1990] and *Fox* [1993] have accounted for the different channels by which the dissociative recombination can occur. Theoretical and experimental work on the hot O corona of Venus has been performed by *Mahajan et al.* [1992], *Nagy and Cravens* [1988], and *Nagy et al.* [1981], and reviewed by *Nagy et al.* [1990].

Recently, *Richards et al.* [1994a] have demonstrated that there is a large number (22) of previously unconsidered sources of geocoronal hot oxygen. Most of these new sources involve reactions of metastable species. The importance of these species (to the present study), established mainly through the Atmosphere Explorer program [*Torr and Torr*, 1982], lies in their ability to transfer electronic energy to translational energy in quenching processes. For example, the metastable $N(^2D)$, which has an electronic energy of 2.4 eV, is produced very efficiently in the thermosphere through direct photodissociation and numerous chemical reactions and is quenched efficiently by atomic oxygen. Electron quenching of $N(^2D)$ was previously found to be an important source of thermal electron heating in the ionosphere by *Richards* [1986], as first suggested by *Dalgarno* [1970]. When $N(^2D)$ is quenched, the electronic

Paper number 95JA00895.
0148-0227/95/95JA-00895$05.00

energy is made available to the translational energy of the two atoms that would then both be hot. The atomic nitrogen atoms may also be produced with translational energy of ~0.1-2 eV [e.g., *Shematovich et al.*, 1991]. (Although collisions with hot N constitute an additional energy source for the ambient O atoms, in this paper we consider only chemical sources, and these important physical processes are not considered). Since the two atoms have approximately the same mass, they will each have more than 1 eV of energy. The energetic N would then transfer its energy to the ambient low-energy O, creating cooler but still hot O atoms. Another possible source of hot O is atomic oxygen quenching of $O^+(^2P)$, which could release up to 5 eV of energy to the two O atoms. Recently, *Chang et al.* [1992] have reevaluated the quenching rate of $O^+(^2P)$ by atomic oxygen and found that it is about 8 times faster than the value derived by *Rusch et al.* [1977].

The calculations of *Richards et al.* [1994a] have demonstrated that quenching of metastable species constitutes a significant source of hot oxygen. For the low-latitude, daytime, wintertime, low magnetic activity, and high solar activity conditions considered by them, some of the most significant new sources of hot oxygen were found to be due to reactions involving quenching of $O^+(^2D)$, $O(^1D)$, $N(^2D)$, $O^+(^2P)$, and vibrationally excited N_2 by atomic oxygen. The kinetic energy production rates due to some of these reactions were found to exceed, by a factor of 10, those due to previously considered O_2^+ and NO^+ dissociative recombination reactions.

The existence of a substantial hot oxygen geocorona is of importance to our understanding of the Earth's atmosphere for several reasons. These include the maintenance of the nighttime ionosphere, the escape flux of He, and energetic ion populations in the plasmasphere. The hot O could help to explain the maintenance of the nighttime ionosphere by increasing the rate of conversion of plasmaspheric H^+ into O^+. At night, H^+ settles out of the plasmasphere into the topside ionosphere and charge exchanges with atomic oxygen. The O^+ then diffuses down to help preserve the nighttime *F* region ion density. Current model calculations, which include ionosphere-plasmasphere coupling, indicate that the flux from the plasmasphere is not sufficient to maintain the ionospheric densities at the observed levels [*Richards et al.*, 1994b]. The existence of enhanced O densities in the topside ionosphere at night would lead to faster conversion of H^+ to O^+ and help to maintain the *F* region at the higher observed densities.

Another possible effect of the hot O geocorona could be to enhance the escape of He atoms from the atmosphere by increasing the population of the high-energy tail of the distribution through collisional energy exchange. The higher exospheric total O density implied by the hot O would also directly increase the He escape flux through charge exchange with atomic oxygen, as has been suggested by *Lie-Svendsen et al.* [1993]. Thus hot O could help to explain the well-known discrepancy between the He outgassing rate and the Jeans escape flux. Finally, the existence of a significant hot O population in the plasmasphere coupled with charge exchange with H^+ could also enhance the population of plasmaspheric O^+ as well as the heating of plasmaspheric ions.

Experimental evidence for the hot oxygen geocorona has been presented by *Yee et al.* [1980] who made twilight measurements of the $O^+(^2P)$ 7320-Å emission. Their measurements indicated a hot oxygen density of up to 10^6 cm^{-3} at 550 km. Further experimental evidence was supplied by *Hedin* [1989]. He inferred hot oxygen densities of 1 to 3×10^4 cm^{-3} at 1100 km for low to moderate solar activities by comparing the satellite drag based (Jacchia) model and the mass spectrometer based (MSIS) model. The satellite drag model assumes that the high-altitude atmosphere consists entirely of helium, while the MSIS model uses information on the composition. The models agree well in winter but are very different in summer, and this difference was attributed to the existence of a hot oxygen geocorona. When extrapolated to 550 km, these inferred densities are in accord with those inferred by *Yee et al.* [1980]. More recently, *Cotton et al.* [1993] have inferred a substantial hot O population from a sounding rocket measurement of the ultraviolet atomic oxygen dayglow.

The hot oxygen production rates of *Richards et al.* [1994a] were calculated for one very specific set of geophysical conditions. The objective of the present study is to determine the variations in these sources of hot oxygen with varying geophysical conditions. The layout of this paper is as follows. First, the numerical model on which the results are based, as well as our assumptions, are discussed in section 2. The results are discussed in three subsections within section 3. Diurnal variations, then latitudinal variations, followed by seasonal and solar cycle variations, are discussed in the first, second, and third subsections, respectively. A discussion of these results is presented in section 4, followed by the conclusions in section 5.

2. Model

The hot oxygen production rates are calculated by using the field line iInterhemispheric plasma (FLIP) transport model [*Richards et al.*, 1994b]. This model solves the coupled time dependent energy, momentum, and continuity equations for the major ions (O^+, H^+, and He^+) and photoelectron transport equations, from 80 km in one hemisphere, along a field line to 80 km in the other hemisphere. The concentrations of the major neutral species are provided by the MSIS-86 model [*Hedin*, 1987]. The main outputs of the FLIP model include ion densities (O^+, $O^+(^4S)$, $O^+(^2D)$, $O^+(^2P)$, H^+, He^+, N^+, NO^+, N_2^+, N_2^{+*}), neutral densities ($N(^4S)$, $N(^2D)$, $N(^2P)$, NO, $O(^1D)$, $O(^1S)$, $N_2(A^3\Sigma_u^+)$, N_2^*), electron and ion temperatures and flow velocities, the photoelectron flux, and a large number of emissions. A recent summary of the FLIP model is provided by *Torr et al.* [1990].

We have identified a total of 27 possible sources of hot oxygen. They are listed in Table 1 and are taken from *Rees* [1989]. The two right-hand columns in Table 1 are the total exothermicity of each reaction and the energy acquired by the product O atom. Note that these acquired energies are taken to be with respect to an initially stationary center of mass for the reactants. The partitioning of energy amongst the products of the reactions was calculated on the basis of conservation of energy and momentum and assumes hard-sphere collisions. Thus the O atom produced in reaction (23), for example, acquires an energy equal to approximately 28/44 ≈ 64% of the available 5.63 eV for the reaction.

Table 1, as presented here, differs from the corresponding table presented by *Richards et al.* [1994a] in several respects. First, reactions (1) and (2) were inadvertently labeled in reverse order by *Richards et al.* [1994a]; this error has been corrected here. Second, here we account for the partitioning of energy between reaction products, as just described. Third, the production rate of hot O due to the quenching of $O(^1D)$ by O was underestimated by a factor of 2 by *Richards et al.* [1994a]; this has been corrected here. Fourth, the $H^+ + O$ reaction is not considered here, for reasons described shortly. Fifth, *Richards et al.* [1994a] considered only one branch of the O_2^+ dissociative

Table 1. Potential Sources of Hot Oxygen and Their Exothermicities (ΔE)

No.	Reaction	Reaction Rate($cm^3\ s^{-1}$)	ΔE_{tot}(eV)	ΔE_O(eV)
(1)	$NO^+ + e \rightarrow N(^2D) + O$	$4.3 \times 10^{-7}(T_e/300)^{-1}$ (78%)	0.38	0.18
(2)	$NO^+ + e \rightarrow N + O$	$4.3 \times 10^{-7}(T_e/300)^{-1}$ (22%)	2.75	1.28
(3)	$O_2^+ + e \rightarrow O + O$	$1.6 \times 10^{-7}(300/T_e)^{0.55}$ (33%)	6.97	3.48
(4)	$O_2^+ + e \rightarrow O(^1D) + O$	$1.6 \times 10^{-7}(300/T_e)^{0.55}$ (21%)	5.02	2.51
(5)	$O_2^+ + e \rightarrow O(^1D) + O(^1D)$	$1.6 \times 10^{-7}(300/T_e)^{0.55}$ (42%)	3.05	1.52
(6)	$O^+ + N(^2D) \rightarrow N(^4S) + O$	$\sim 7 \times 10^{-13}$	2.38	1.11
(7)	$O + O(^1D) \rightarrow O + O$	8×10^{-12}	1.96	0.98
(8)	$O + O^+(^2P) \rightarrow O^+ + O$	4×10^{-10}	5.00	2.50
(9)	$O + O^+(^2D) \rightarrow O^+ + O$	5×10^{-12}	3.31	1.65
(10)	$N(^2D) + O^+ \rightarrow N^+ + O$	5×10^{-11}	1.46	0.68
(11)	$O_2 + O^+ \rightarrow O_2^+ + O$	$2.1 \times 10^{-11}\{T_n + 2T_i/3 \times 300\}^{-0.763}$	1.55	1.03
(12)	$N_2 + O^+(^2D) \rightarrow N_2^+ + O$	8×10^{-10}	1.33	0.85
(13)	$O(^1D) + N_2 \rightarrow O + N_2$	$2.0 \times 10^{-11}\exp(107.8/T)$	1.31	0.84
(14)	$N(^2D) + O_2 \rightarrow NO + O$	6×10^{-12}	3.76	2.45
(15)	$N(^2P) + O \rightarrow N + O$	1.7×10^{-11}	3.58	1.67
(16)	$NO + N \rightarrow N_2 + O$	3.4×10^{-11}	3.25	2.07
(17)	$N + O_2 \rightarrow NO + O$	$4.4 \times 10^{-12}\exp(-3220/T)$	1.385	0.90
(18)	$N^+ + O_2 \rightarrow NO^+ + O$	2×10^{-10}	6.67	4.35
(19)	$O^+(^2D) + O_2 \rightarrow O_2^+ + O$	7×10^{-10}	4.865	3.24
(20)	$O^+(^2P) + N_2 \rightarrow N_2^+ + O$	4.8×10^{-10}	3.02	1.92
(21)	$O(^1D) + O_2 \rightarrow O_2^+ + O$	$2.9 \times 10^{-11}\exp(67.5/T)$	1.96	1.31
(22)	$O_2^+ + N \rightarrow NO^+ + O$	1.2×10^{-10}	4.2	2.74
(23)	$NO + N(^2D) \rightarrow N_2 + O$	7×10^{-11}	5.63	3.58
(24) - (27)	$N_2^*(v) + O \rightarrow N_2(v'=0) + O$	*McNeal et al.* [1974]	0.3v	0.19v

recombination reaction and assumed the hot O to be produced with the average energy of the several known branches. Here, we correctly account for the three most energetic and important branches for this reaction. We do so by assuming, like *Yee* [1988], that the two most energetic branches producing $O(^1D)$ occur with equal probability. Each O_2^+ dissociative recombination reaction is assumed to produce 1.3 $O(^1D)$ atoms [*Abreu et al.*, 1986] and 0.08 $O(^1S)$ atoms [e.g., *Torr et al.*, 1990]. We also assume, like *Rohrbaugh and Nisbet* [1973], that the two branches producing $O(^1S)$ occur with equal probability. There is some evidence that the yield of the $O(^1S)$ + $O(^3P)$ channel is negligible [*Guberman and Giusti-Suzor*, 1991]. However, neither of these two channels is considered in our final results because their yields are small. Using these values produces the branching ratios given in Table 1.

As discussed by *Richards et al.* [1994a], in some reactions involving molecular products, the energy partitioning is complicated by possible electronic and vibrational excitation of the molecule. For example, reaction (12) ($O^+(^2D) + N_2 \rightarrow O + N_2^+$) may result in the excitation of the $N_2^+(A)$ state [*Omholt*, 1957], in which case most of the energy will be radiated. Alternatively, the reaction may produce $N_2^+(X)$ in vibrational levels up to v = 5. In this case, O quenching of the vibrational levels may lead to a significant source of hot O. Spectroscopic measurements made on the ATLAS 1 mission indicate significant production of $N_2^+(X)$, with little or no production of $N_2^+(A)$ [*Torr et al.*, 1993]. However, the chemistry of vibrationally excited N_2^+ has not yet been fully quantified. Previously [*Richards et al.*, 1994a], we did not consider the vibrational excitation of molecular products for any of the reactions studied. Here, and for reaction (13) only, we assume that 33% of the available exothermic energy appears as vibrational energy of N_2 [*Slanger and Black*, 1974]. We realize that smaller values of exothermicity should be considered for some of the other reactions in Table 1 involving molecular products due to their possible vibrational excitation. However, the uncertainties associated with this precludes our doing so, and we simply note that for some of those reactions involving molecular products the exothermicities employed here may be overestimated by as much as approximately 50% and they therefore represent an upper limit. For some of the reactions involving only monatomic products, the possibility that one of the atoms is electronically excited would also imply that the exothermicity is overestimated. This may be the case for reactions (8) and (15), for example, in which $O^+(^2D)$ and $N(^2D)$ may be formed, respectively. We do not consider electronic excitation of atomic products here, but again note that we may be overestimating the exothermicity for some of these reactions.

Reactions (1) to (5) have been previously examined as a source of geocoronal hot oxygen by *Rohrbaugh and Nisbet* [1973]. The charge exchange of O^+ with H was considered by *Richards et al.* [1994a] as a source of hot geocoronal oxygen, and was previously considered by *Nagy et al.* [1981] for the ionosphere of Venus. However, the energy for the hot O derives from the initial O^+ kinetic energy and not from the conversion of chemical energy. For this reason, this reaction is not considered here. Reactions (24) to (27) correspond to N_2^* vibrational levels (v) ranging from 1 to 4, respectively. For these quenching reactions we employed the reaction rate coefficients of *McNeal et al.* [1974] and applied them according to *Newton et al.* [1974]. We assume that quenching is to the ground vibrational level, which is unlikely for $v \geq 2$, and implies that our results for this reaction constitute an upper bound for the production of hot O kinetic energy.

In this study we are primarily interested in comparing the new sources of hot oxygen with the previously known sources (reactions (1) to (5)) in order to demonstrate the potential importance of these new sources. We emphasize that it is the local production of hot oxygen that is calculated here. The final dis-

tribution of hot oxygen atoms will depend on collisions and transport, and its calculation is beyond the scope of this paper. Transport, primarily responsible for populating the exosphere, becomes more important in the vicinity of the exobase where the mean free path of an O atom becomes comparable to its scale height. The height of the exobase is highly variable, having diurnal, seasonal, and solar cycle variations. In the results soon to be described, we find that the daytime exobase height ranges from about 370 km for low solar activity to about 520 km for high solar activity. Transport will become important within about a scale height (~50-80 km) of the exobase, which for the conditions just described will be somewhere above approximately 320 km to 440 km. At lower altitudes where collisions are more frequent, the hot O will be quickly thermalized, and will primarily contribute to the local thermospheric heat budget without contributing to the hot O geocoronal population. For this reason, we place more emphasis on the high-altitude production of hot O. For completeness, however, we present results for all altitudes.

3. Results

The FLIP model was run for summer and winter conditions (days 1 and 160, respectively), different levels of solar activity ($F_{10.7}$ = 80 and 200), for local times close to midnight (LT ≈ 0.28 hours) and midday (LT ≈ 12.88 hours), and for two latitudes (~ 18°N and ~42.6°N). A longitude of about 70°W and a low level of magnetic activity (Ap = 12) were used. The model was run for an initial period of 24 hours prior to these times, in order to reduce dependence on initial conditions.

The results of our calculations are presented in the following three subsections, where we examine the diurnal variations of all 27 possible sources of hot oxygen for daytime, summer, high solar activity conditions; the latitudinal variations of these sources, also for daytime, summer, high solar activity conditions; and the seasonal and solar cycle variations of only the most significant sources of hot oxygen for daytime, low-latitude conditions. We also calculate hot O source energy spectra as a function of altitude, and show how they vary with season and solar cycle. For the first subsection we also present the neutral and ionic species' number densities output from the FLIP model that were used to calculate the hot O production rates. This helps to provide a physical explanation for the diurnal variation of hot O production. For conciseness we do not present these species' number densities for the remaining variations, but merely note that their variations are reflected in the hot O production rate variations.

The FLIP model calculates the metastable species' densities, assuming that local chemical equilibrium prevails. This is a good assumption at low altitudes, but breaks down at high altitudes where collisions are infrequent and transport becomes important. Therefore we do not present hot O production rates for altitudes above approximately 520 km. For the remainder of this paper, we will represent the hot O number density production rate due to each reaction by η, and the hot O kinetic energy production rate due to each reaction by ε.

Diurnal Variations

The hot O production rates were calculated for summer (day 160), moderately high solar activity ($F_{10.7}$ = 200) conditions at a latitude of ~18°N, for local times close to midnight (LT ≈ 0.28 hours) and midday (LT ≈ 12.88 hours).

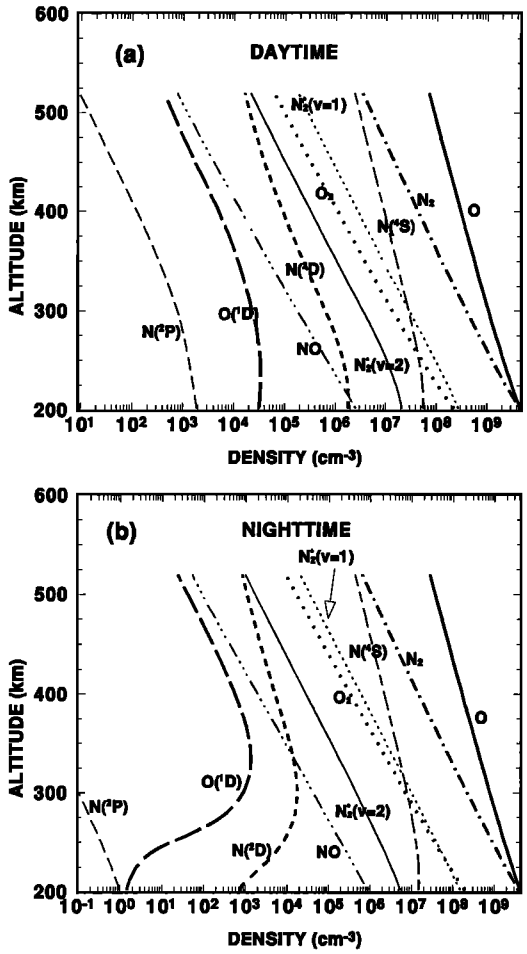

Figure 1. Neutral species' (a) daytime (LT ≈ 12.88 hours) and (b) nighttime (LT ≈ 0.28 hours) densities for low-latitude, summer, moderately high solar activity conditions.

First, we present the daytime and nighttime species number densities that were used in the calculation of hot O production rates. All daytime neutral densities (Figure 1a) are greater than their nighttime values (Figure 1b). Nighttime densities of O, N_2, and O_2 are approximately half their daytime values at the highest altitudes, with smaller variations occurring at lower altitudes. The magnitude of the diurnal density variation for most other species is between 1 and 2 orders of magnitude. Most daytime ion and electron densities (Figure 2a) are greater than their nighttime values (Figure 2b), except at high altitudes where the daytime and nighttime values of the electron, N^+, and O^+ densities are comparable. The nighttime densities of the minor metastable ions $O^+(^2D)$ and $O^+(^2D)$ are more than 4 orders of magnitude smaller than their daytime values at all altitudes. In contrast, the nighttime densities of O_2^+ and NO^+ are only about 1 order of magnitude smaller than their daytime values. Therefore, while at high altitudes the densities of $O^+(^2P)$ and $O^+(^2D)$ are comparable to or greater than NO^+ and O_2^+ densities during daytime, at night the $O^+(^2P)$ and $O^+(^2D)$ densities are very small by comparison.

The volume production rates, η, derived from the set of chemical reactions given in Table 1 are plotted as a function of altitude for daytime (Figure 3) and nighttime (Figure 4). For clarity of presentation, the results have been separated into three groups, the first containing reactions (1) to (9), the second

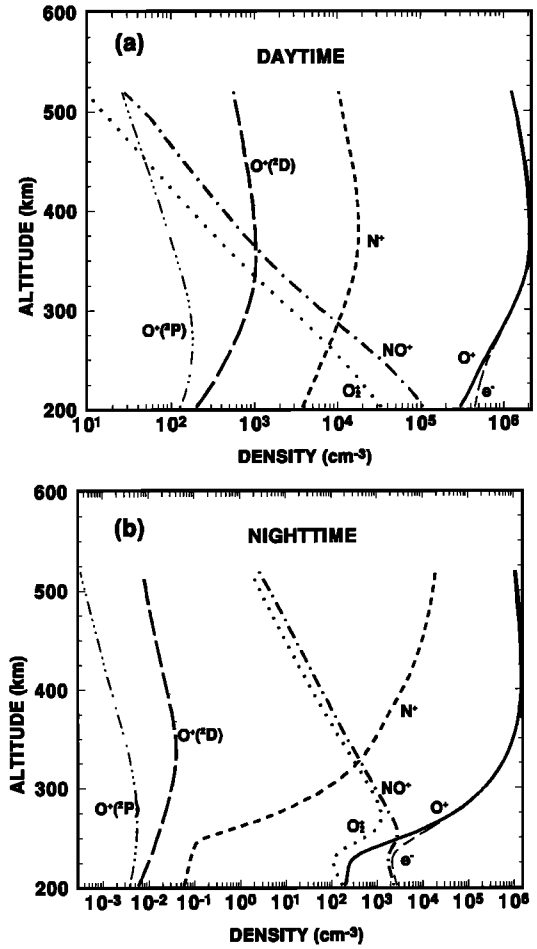

Figure 2. Ion and electron species' (a) daytime (LT ≈ 12.88 hours), and (b) nighttime (LT ≈ 0.28 hours) densities for low-latitude, summer, moderately high solar activity conditions.

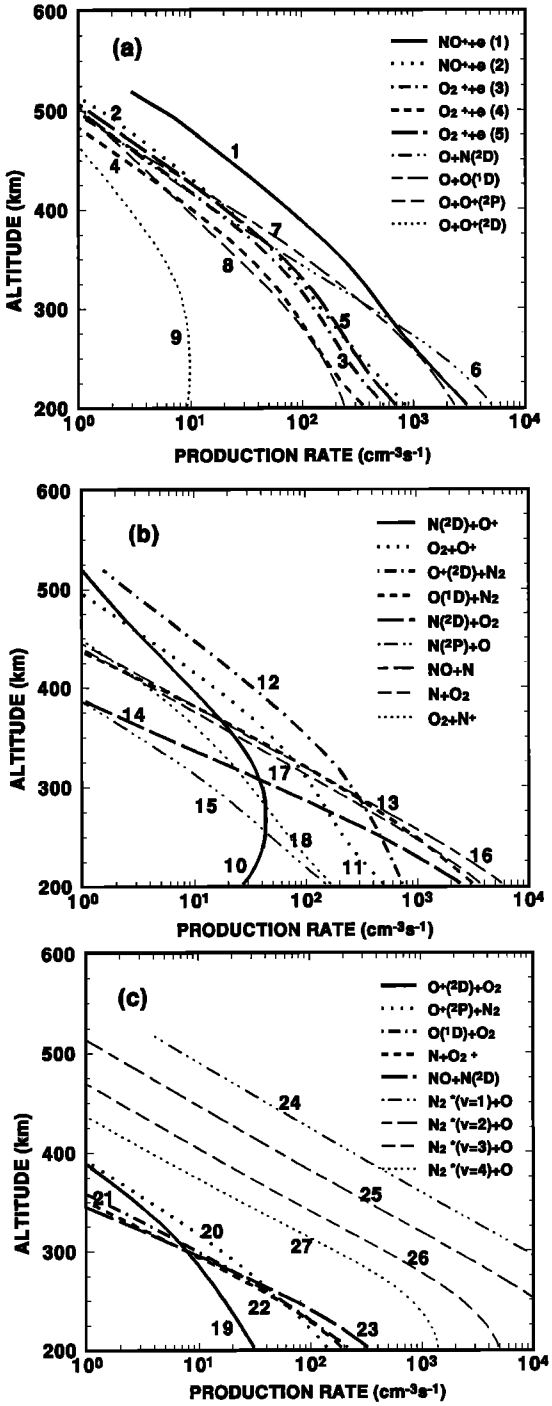

Figure 3. Daytime (LT ≈ 12.88 hours) hot O volume production rates at 18°N for summer, high solar activity for reactions (a) (1) to (9), (b) (10) to (18), and (c) (19) to (27).

containing reactions (10) to (18), and the third containing reactions (19) to (27). For comparison purposes we note that the exobase altitudes are approximately 520 km and 452 km under these conditions for the daytime and nighttime models, respectively. The daytime η values are dominated by quenching of $N_2^*(v = 1)$ by atomic oxygen (reaction (24)) at all altitudes (Figure 3c). At these highest altitudes, dissociative recombination of NO^+ (reaction (1)) becomes of comparable importance. The $O^+(^2D)$ charge transfer with N_2 (reaction (12)) is also an important source of hot oxygen at high altitudes. At the highest altitudes, a number of less important sources of hot oxygen production rates are due to reactions (2), (3), (4), (5), (6), (7), (8), (10), (11), and (25), as shown in Figure 3.

The nighttime values of η (Figure 4) are generally at least an order of magnitude smaller than their corresponding daytime values. This is not surprising, given the large daytime values of reacting species' densities compared to their nighttime values (Figures 1 and 2). Furthermore, while $O^+(^2D)$ may be a significant source of daytime hot O through reaction (12) (Figure 3b), it is nonexistent at night (Figure 4b). The values of η are dominated by quenching of $N_2^*(v = 1)$ by atomic oxygen (reaction (24)) below about 425-km altitude (Figure 4c), and by the dissociative recombination of NO^+ (reaction (1)) above 425 km (Figure 4a). At high altitudes the dissociative recombination of O_2^+ (particularly reactions (3) and (5)) and the charge transfer reaction between O^+ and O_2 (reaction (11)) are also important in the production of hot O (Figure 4b). Below about 300-km altitude, quenching of N_2^* (reactions (24) to (27)), as well as the atom-atom interchange reactions (16) and (17), dominate the production of hot O (Figures 4b and 4c).

While values of η are useful indicators of which sources may be of significance to the hot O population, the kinetic energy production rates ($\mathcal{E}$) are of greater interest because they are a direct measure of the available kinetic energy for the product oxygen atom. These values of $\mathcal{E}$ (Figures 5 and 6) were obtained

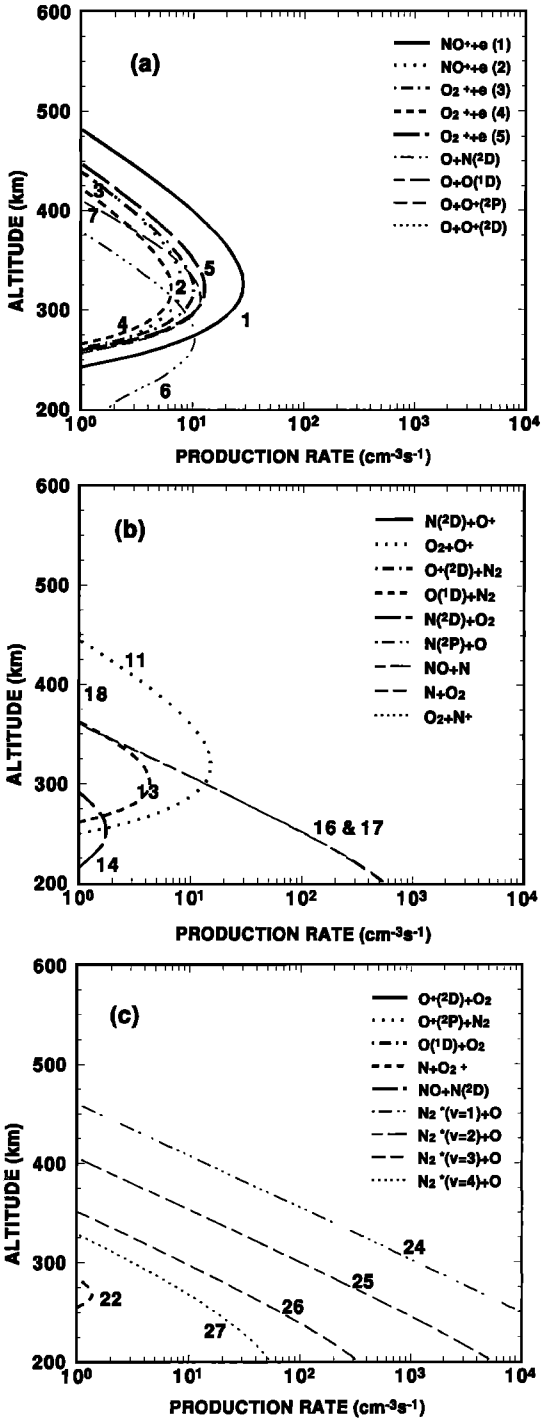

Figure 4. Nighttime (LT ≈ 0.28 hours) hot O volume production rates at 18°N for summer, high solar activity for reactions (a) (1) to (9), (b) (10) to (18), and (c) (19) to (27).

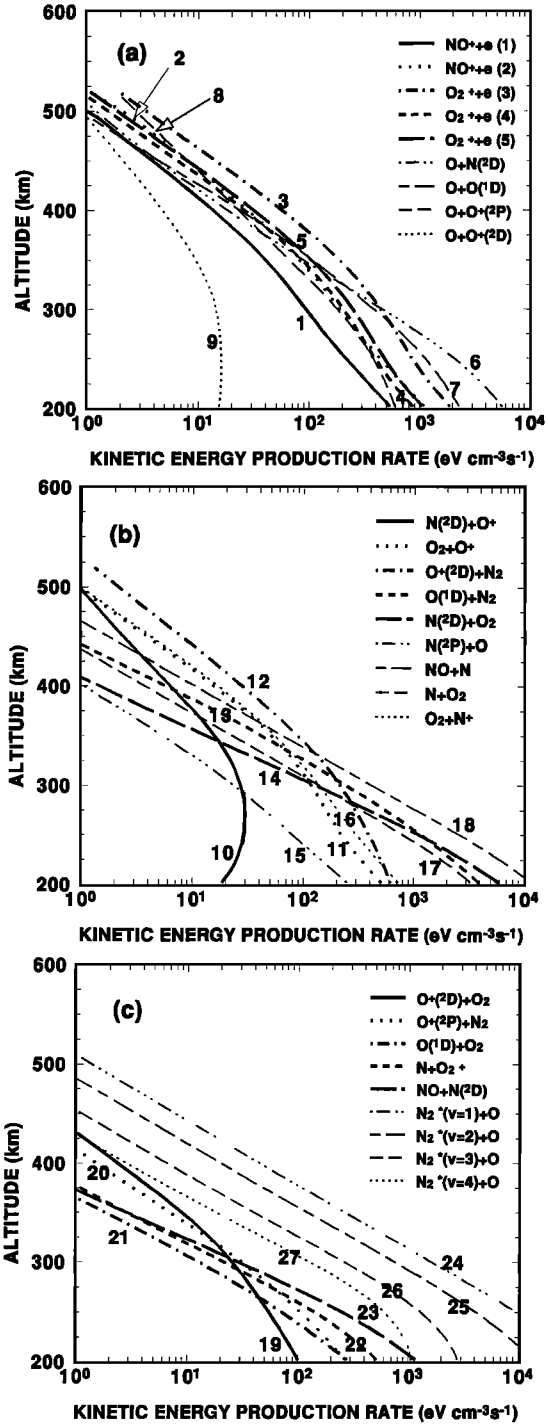

Figure 5. Daytime (LT ≈ 12.88 hours) hot O kinetic energy production rates at 18°N for summer, high solar activity for reactions (a) (1) to (9), (b) (10) to (18), and (c) (19) to (27).

by multiplying the hot O number density production rate by the kinetic energy acquired by a single O atom for each reaction in Table 1.

The daytime results for summer at solar maximum presented in Figures 5a, 5b, and 5c show that dissociative recombination of O_2^+ (reaction (3)) dominates $\mathcal{E}$ at altitudes above about 375 km, while quenching of N_2^* (reaction (24)) dominates below that. Atomic oxygen quenching of $O^+(^2P)$ (reaction (8)) produces large values of $\mathcal{E}$ at the highest altitudes and is slightly more important than the dissociative recombination reaction (2) of NO^+ (Figure 5a). Other important sources of $\mathcal{E}$ at high altitudes include charge transfer between $O^+(^2D)$ and N_2 (reaction (12)), quenching of $N(^2D)$ by O (reaction (6)), dissociative recombination of NO^+ (reaction (2)), and the dissociative recombination of O_2^+ through reactions (4) and (5).

As with the volume production rates ($\mathcal{P}$), the nighttime values of $\mathcal{E}$ (Figure 6) are significantly smaller than their corresponding daytime values. Also, $O^+(^2P)$ (reaction (8)) and $O^+(^2D)$ (reaction (12)) are not sources of hot O at night (Figures 6a and 6b), as might be expected from their diurnal density variation. At

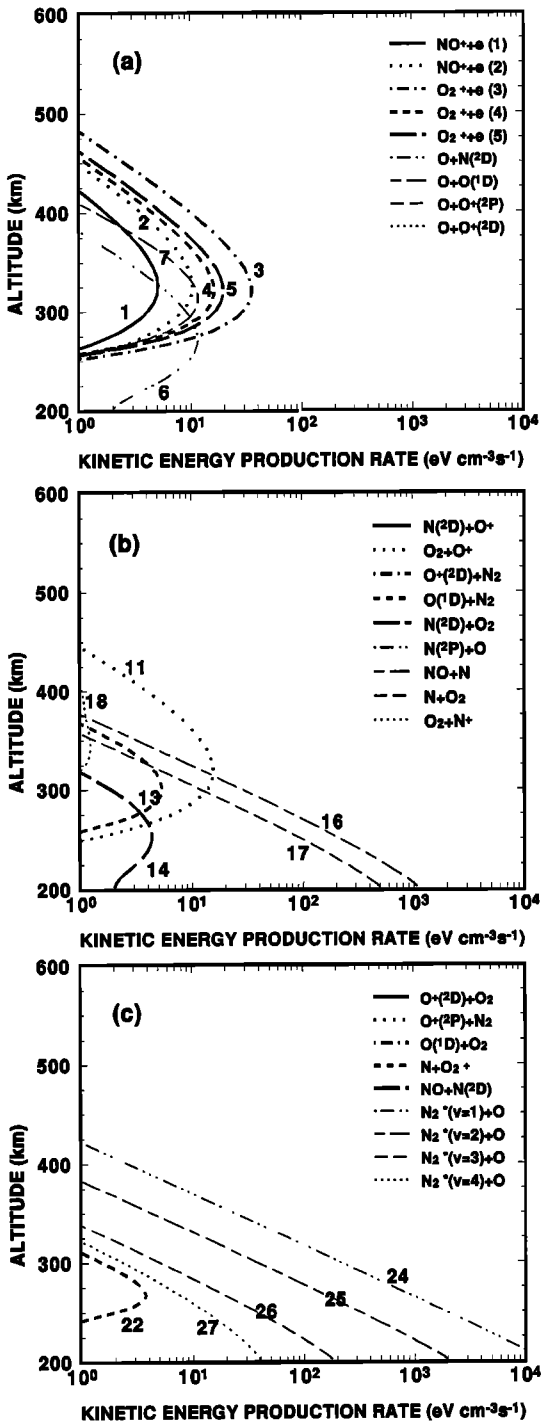

Figure 6. Nighttime (LT ≈ 0.28 hours) hot O kinetic energy production rates at (18)°N for summer, high solar activity for reactions (a) 1 to (9), (b) (10) to (18), and (c) (19) to (27).

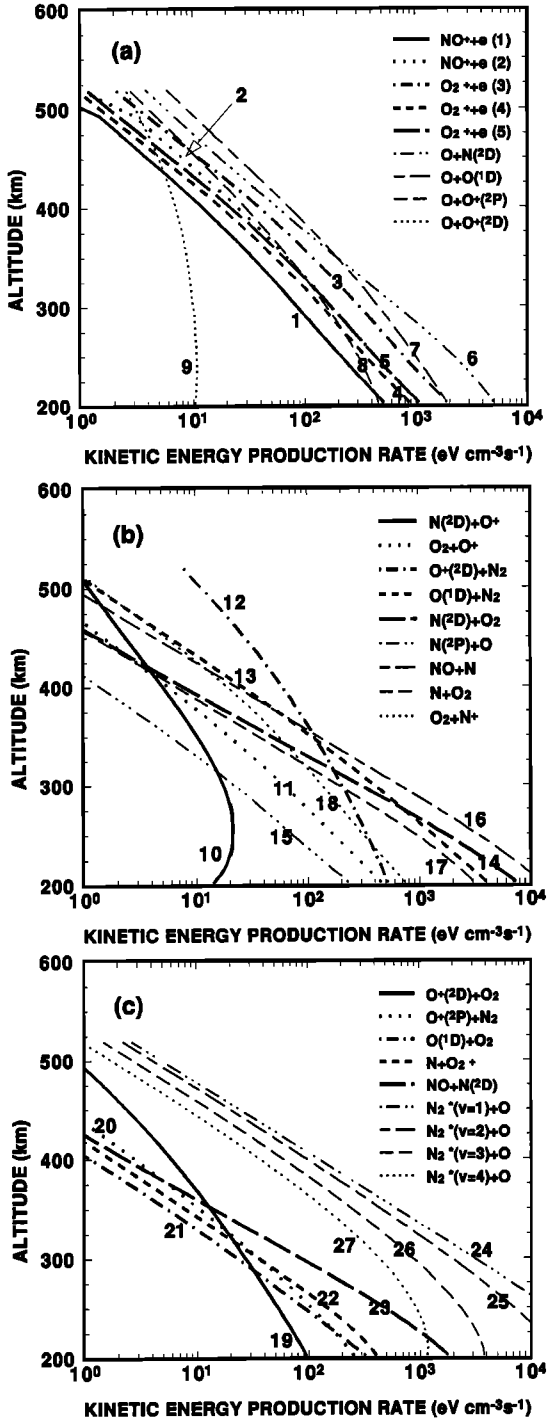

Figure 7. Daytime (LT ≈ 12.88 hours) hot O kinetic energy production rates at 42.6°N for summer, high solar activity for reactions (a) 1 to (9), (b) (10) to (18), and (c) (19) to (27).

altitudes above about 400 km the important sources of $\mathcal{E}$ at night are due to dissociative recombination of O_2^+ and NO^+ (reactions (1) to (5)), reaction (11), and quenching of N_2^* ($v = 1$) by O (reaction (24)), with smaller contributions coming from reactions (7) and (18).

Latitudinal Variations

To show latitudinal variations, the production of hot O was calculated for daytime (LT ≈ 12.88 hours), summer (day 160), moderately high solar activity ($F_{10.7} = 200$) conditions at 42.6°N, and compared with the results for 18°N shown in Figure 5. Under these conditions the exobase altitude is approximately 520 km for both latitudes. In this section, we concentrate on the hot O kinetic energy production rates ($\mathcal{E}$) because these are generally of more aeronomical significance.

Values of $\mathcal{E}$ for 42.6°N are shown in Figure 7. Quenching of N_2^*($v = 1$ and 2) by O dominates $\mathcal{E}$ up to altitudes of about 450 km, and exceeds the combined values of $\mathcal{E}$ for reactions (1), (2), (3), (4) and (5) at all altitudes. At higher altitudes several reactions involving quenching of metastable species dominate (see

Figures 7a and 7b). Among these are reactions (12), (6), (7), (8), and (9), with reactions (24) and (25) also making significant contributions. Of the dissociative recombination reactions, the most important at high altitudes is reaction (3). These midlatitude results are quite different from the low latitude results shown in Figure 5, in which the high-altitude production of hot O kinetic energy was dominated by the dissociative recombination of O_2^+ (reaction (3)).

The major differences between hot O kinetic energy production rates produced at the low and middle latitudes can be summarized as follows. At any altitude, the low-latitude values of $\mathcal{E}$ due to the dissociative recombination of NO^+ and O_2^+ are very similar to their midlatitude values. By contrast, values of $\mathcal{E}$ due to all of the new sources of hot O display a large increase from the low to the high latitudes. The only exception to this occurs at low altitudes, where increases in $\mathcal{E}$ are typically smaller between the two latitudes, and where the low-latitude values of $\mathcal{E}$ due to reactions (7) and (9) are greater than their middle-latitude values. At high altitudes the midlatitude value of $\mathcal{E}$ due to reaction (7) is about 10 times greater than its low-latitude value. The high-altitude increases between the two latitudes obtained for the other new sources of hot O are more modest, but typically range between factors of 2 and 5.

These latitudinal variations in the hot O production rates can be explained in terms of the latitudinal variations of the neutral and ion species densities. There is significantly more $O(^1D)$, $N(^2D)$, NO, $N_2^*(v = 1, 2)$, $O^+(^2D)$ and NO^+ above ~300 km at midlatitudes than at low latitudes. However, there is less N^+ and O^+ and fewer electrons at midlatitudes than at low latitudes. Thus, while hot O production is increased at the midlatitude due to increases in the metastable species densities, there is little latitudinal variation in hot O production due to ion dissociative recombination because the effects of an increase in ion density are counteracted by the effects of a decrease in the electron density.

Seasonal and Solar-Cycle Variations

In this section, the production of hot O was calculated for daytime (LT ≈ 12.88 hours), low-latitude (18°N) conditions, for both winter (day 1) and summer (day 160), and for both low ($F_{10.7}$ = 80) and moderately high ($F_{10.7}$ = 200) solar activity. Under these conditions and for a given level of solar activity the exobase altitudes are comparable for summer and winter. For low solar activity the exobase altitudes are approximately 377 km (winter) and 370 km (summer), while for moderately high solar activity they are approximately 520 km for both winter and summer.

For each set of results we selected the 10 reactions that provided the largest hot O kinetic energy production rates ($\mathcal{E}$) at the highest altitudes. The decision to select sources based on their values at high altitudes was motivated by the fact that at higher altitudes the hot O produced is less likely to be collisionally thermalized, and, all other things being equal, will have a much greater probability of populating the geocorona. At lower altitudes where collisions dominate, the hot O will be quickly thermalized, and will primarily contribute to the local thermospheric heat budget without contributing to the hot O geocoronal population. The particular set of 10 reactions selected depends on season and solar cycle. It is important to note that the selection of the largest sources based on their high-altitude values means that sources which may be totally dominant at lower altitudes, such as those associated with quenching of N_2^* (reactions (24) to (27)), may not appear in the following figures. However, these sources will be given due consideration later in this section. Again, we concentrate on the hot O kinetic energy production rates ($\mathcal{E}$) because these are generally of more aeronomical significance.

The hot O kinetic energy production rates ($\mathcal{E}$) are shown in Figure 8. The values of $\mathcal{E}$ for winter at low solar activity (Figure 8a) reveal that at the highest altitudes (above 350 km) reactions (9), (12), (6) and (8) dominate over the O_2^+ and NO^+ dissociative recombination reactions ((1) to (5)). Above 400-km altitude the hot O energy derives almost exclusively from $O^+(^2D)$. Although reaction (9) produces negligible values of $\mathcal{E}$ at low altitudes, it is a major source at high altitudes. Quenching of $O(^1D)$ by O is only an important source of $\mathcal{E}$ at lower thermospheric altitudes. These wintertime, low solar activity results have been previously discussed by *Richards et al.* [1994a], where, however, no account was taken of the partitioning of energy between the various reaction products.

Values of $\mathcal{E}$ for winter at high solar activity (Figure 8b) also show that reaction (9) is a major source of hot O at high altitudes, but is a negligible source at low altitudes. Reaction (7) dominates $\mathcal{E}$ between about 400-km and 500-km altitude, beyond which reaction (12) dominates. Quenching of $N(^2D)$ and $O^+(^2P)$ by O (reactions (6) and (8)) are also important sources of $\mathcal{E}$ at high altitudes. Quenching of vibrationally excited N_2 by O (reactions (24) and (25)) is at least as important as the dissociative recombination reactions of O_2^+ and NO^+ (reactions (2) and (3)) as a source of kinetic energy for the hot O at high altitudes, but none of these compares to the previously noted sources.

Figure 8c shows values of $\mathcal{E}$ for summer at low solar activity. Quenching of $N(^2D)$ by O (reaction (6)) dominates at most altitudes, with comparable contributions being due to reactions (3) and (12) at the highest altitudes. The dissociative recombination of NO^+ (reaction (2)) is a minor source of hot oxygen under these conditions. An interesting feature of these results is that near 400-km altitude and for low solar activity the hot O kinetic energy production rates for summer (Figure 8c) are smaller than those for winter (Figure 8a).

Figure 8d shows values of $\mathcal{E}$ for summer at high solar activity. At high altitudes the dissociative recombination of O_2^+ (reaction (3)) dominates, although quenching of $O^+(^2P)$ by O (reaction (8)) appears to be equally important at the highest altitudes (above 500-km). Other important sources at high altitudes are due to reactions (2), (5), and (12). At low altitudes, quenching of N_2^* and $N(^2D)$ by O (reactions (24) and (6)) dominate (see Figure 5b). At altitudes near 500-km and for high solar activity the hot O kinetic energy production rates for summer (Figure 8d) are smaller than those for winter (Figure 8b).

The hot O kinetic energy production rates discussed in this subsection can be summarized as follows. First, reaction (12), $(N_2+O^+(^2D))$, is one of the most important reactions for the production of hot O, usually being one of the three largest sources of $\mathcal{E}$. Dissociative recombination of O_2^+, mainly due to reaction (3), is the largest source of $\mathcal{E}$ only during summer at high solar activity, and the second largest source during summer at low solar activity. During winter it is a less significant source. Dissociative recombination of NO^+ (reaction (2)) is only a major source of $\mathcal{E}$ during summer at high solar activity. At other times it is a less significant source. Quenching of $O^+(^2D)$ by O (reaction (9)) is a major source of $\mathcal{E}$ only at high altitudes during winter, irrespective of the level of solar activity. Quenching of $N(^2D)$ by O (reaction (6)) is one of the most important sources of

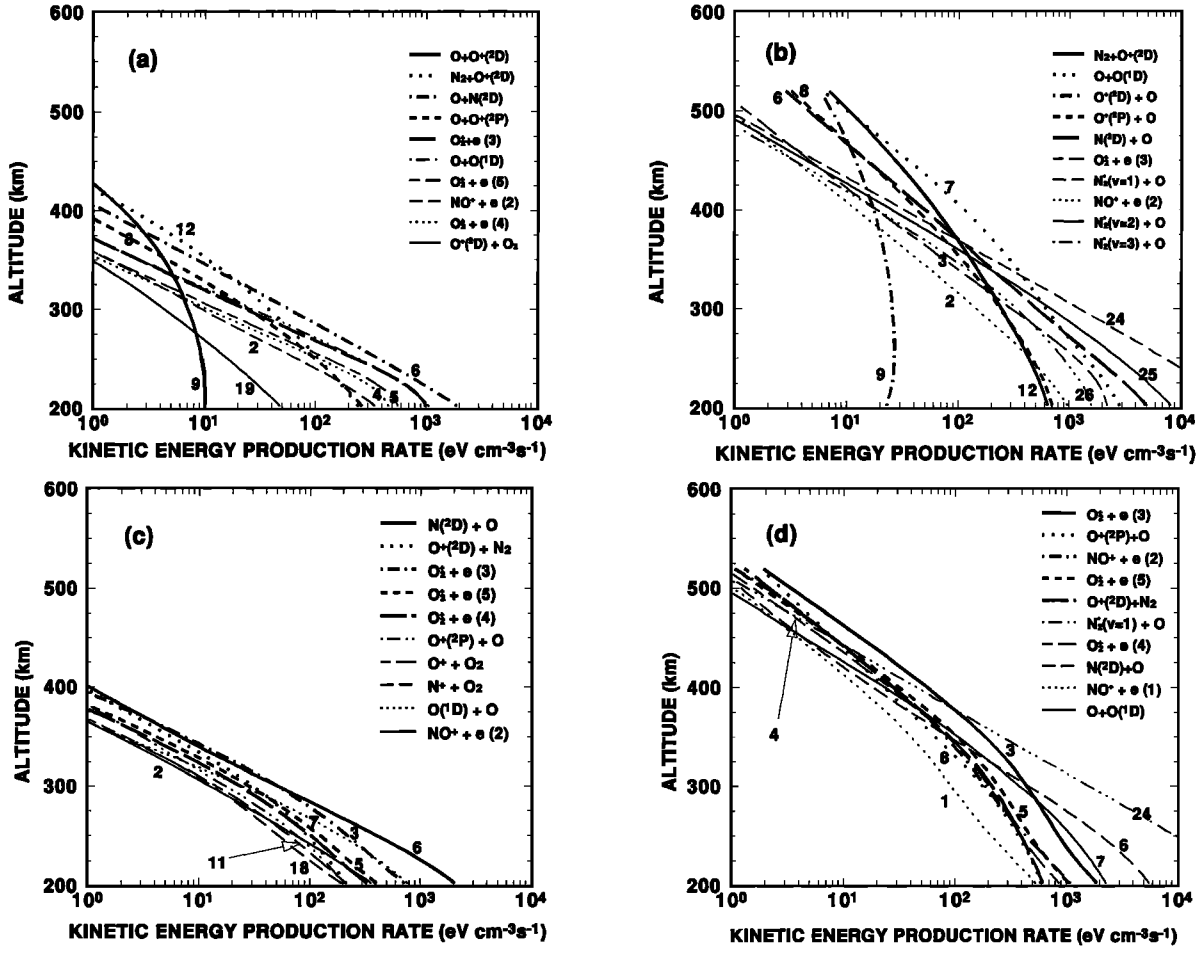

Figure 8. Daytime (LT ≈ 12.88 hours) hot O kinetic energy production rates at (18)°N for (a) winter, low solar activity, (b) winter, high solar activity, (c) summer, low solar activity, and (d) summer, high solar activity. Note that only the ten largest sources are included (see text for details).

$\mathcal{E}$ during winter, and is the largest source during summer at low solar activity. It is a less important source during summer at high solar activity. Quenching of $O^+(^2P)$ by O (reaction (8)) is overall an important source of $\mathcal{E}$, for any season or level of solar activity. Quenching of $O(^1D)$ by O (reaction (7)) is only a significant source of $\mathcal{E}$ during winter for high solar activity. Quenching of $N_2^*(v = 1$ and 2) by O (reactions (24) and (25)) is only a significant source of $\mathcal{E}$ at high solar activity and is more important at altitudes below about 375 km. It is not a significant source at low solar activity.

We find that the hot O kinetic energy production rates at high altitudes increase with increasing solar activity for both summer and winter. However, an important result discovered here is that for a fixed level of solar activity these production rates are larger in winter than in summer. This seasonal variation in the production of hot O kinetic energy is due to the seasonal variation in the new, metastable sources of hot O considered here. In contrast, the production rates due to the dissociative recombination reactions shown in Figure 8 are smaller in winter than in summer for a given level of solar activity.

In addition to examining the hot O kinetic energy production rates, it is also of interest to examine the energy distribution of the hot O sources. As previously stated, the energy partitioning of the reaction products was calculated following conservation of energy and momentum principals, and provided us with the hot O source kinetic energy for each reaction as provided in the right-hand column of Table 1. These energies lay in the range of about 0.18 to 4.35 eV. Energy spectra were defined by using 22 energy bins ranging from 0 to 4.4 eV, each bin being 0.2 eV wide. For each energy bin the total hot O number density production rate was calculated by summing the individual hot O volume production rates for all reactions contributing energy to that bin. Then the energy spectrum was normalized by dividing the hot O production rate for each bin by the total hot O production rate. These normalized hot O kinetic energy source spectra were generated at every altitude. Note that these spectra, by definition, are independent of the total hot O production rate at any altitude.

We present results for the seasonal and solar cycle variations of the hot O kinetic energy source spectra in Figure 9. We have truncated the spectra at 3.6 eV because at higher energies the relative production rates are generally rather small and uninteresting. The only reactions that create hot O more energetic than 3.6 eV are reactions (18) (4.35 eV), (19) (3.24 eV), and (23) (3.58 eV). Of these, the most important is reaction (18). However, even for this reaction the relative production rates only become discernible at altitudes near 500 km during summer, being negligible otherwise.

Figure 9a shows the normalized hot O kinetic energy source spectra as a function of altitude for winter and low solar activity.

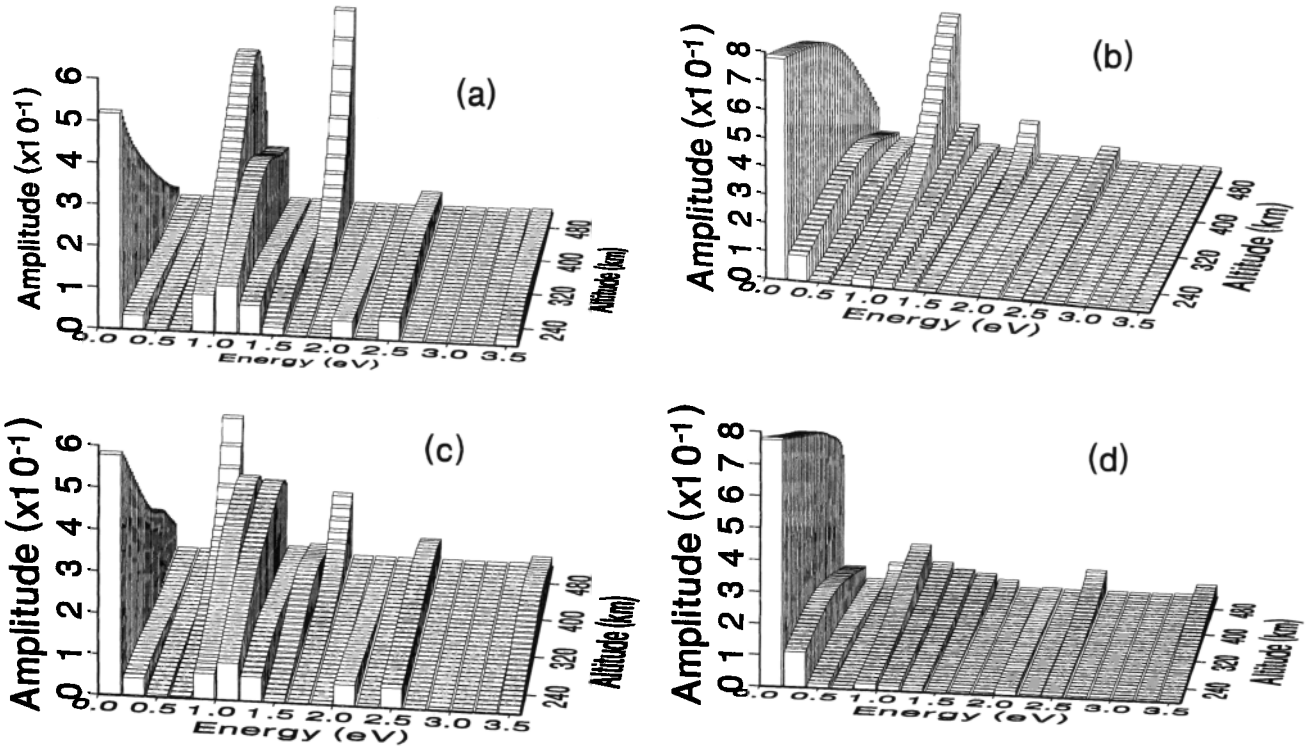

Figure 9. Daytime (LT ≈ 12.88 hours) hot O kinetic energy source spectra versus altitude at (18)°N for (a) winter, low solar activity, (b) winter, high solar activity, (c) summer, low solar activity, and (d) summer, high solar activity. At each altitude the amplitude spectrum is normalized so that the sum of amplitudes over all energies is unity. Note that spectra are derived from binning the production rates in 0.2-eV intervals.

A number of features are evident. First, the energy source is not distributed uniformly, but is of course discrete. At the lowest altitudes an appreciable fraction (~55%) of the hot O appears to be created with energies below 0.2 eV (due mainly to reaction (24) with some due to reaction (1)). At these altitudes there is a small fraction of hot O created with energies between 0.2 and 0.4 eV (due to reaction (25)), about 30% created with energies between 0.8 and 1.4 eV (due mainly to reactions (12), (6), and (2)), with the remaining between 2.0 and 3.6 eV (due mainly to reactions (16), (4), (8), and (3)). Proceeding to higher altitudes, the lowest-energy sources (reactions (24) and (1)) decrease and become small by 500-km altitude. Between 0.8 and 1.0 eV, hot O production rates (mainly due to reaction (12) at higher altitudes) increase with increasing altitude (relative to the total), reaching a maximum in the vicinity of about 400-km altitude, and decreasing thereafter. Hot O production rates at energies between 1.0 and 1.2 eV increase (relative to the total) with increasing altitude, peaking near 300 km, and decreasing again thereafter. Hot O production rates at energies between 1.6 and 1.8 eV (due to reaction (9)) increase dramatically (relative to the total) with increasing altitude, and totally dominate the hot O spectrum at high altitudes (see also Figure 8a). However, one needs to be reminded that at altitudes above about 400 km the total hot O production rates become small under these low solar activity conditions. For the remaining energies, hot O production rates either decrease or remain approximately constant with increasing altitude.

Figure 9b shows the normalized hot O kinetic energy source spectra as a function of altitude for winter and high solar activity. At low altitudes the spectrum is dominated (~80%) by the lowest energies available to hot O production (0.19 eV) due to reaction (24). Hot O production rates at this low energy decrease slowly with increasing altitude, and still make a significant contribution to the spectrum at the highest altitudes. At the lowest altitudes, reaction (25) is responsible for producing about 10% of the hot O with energies of 0.38 eV. The relative production rates at this energy initially increase slightly with increasing altitude, and then decrease at the highest altitudes. Hot O production rates between 0.8 and 1.0 eV (reactions (7) and (12)) increase dramatically with increasing altitude, dominating the spectrum at the highest altitudes. The large increase in the normalized hot O production rates at energies of 1.6 to 1.8 eV (reaction (9)) seen at high altitudes and low solar activity (Figure 9a) is not as pronounced at high solar activity (Figure 9b). This can also be seen by comparing Figure 8a with Figure 8b.

Figure 9c shows the normalized hot O kinetic energy source spectra as a function of altitude for summer and low solar activity. At low altitudes the low-energy portion of the spectrum resembles that shown in Figure 9a. For energies between 0.6 and 0.8 eV there is a large increase in the normalized hot O production rates with increasing altitude due to the increased importance of reaction (10); these energies dominate the spectrum above about 500-km altitude (recall, however, that at high altitudes the total hot O production rates are very small under low solar activity conditions). Between 0.8 and 1.2 eV, normalized hot O production rates increase, due mainly to reactions (12) and (6). Between 1.2 and 1.4 eV, normalized hot O production rates due to reaction (2) remain approximately constant with increasing altitude up to about 300-km altitude, and decrease slowly

thereafter. There is an increase at the highest altitudes in normalized hot O production rates for energies between 1.6 and 1.8 eV (reaction (12)) that are not as pronounced as those for winter at low solar activity (Figure 9a). At energies between 2.0 and 2.6 eV, normalized hot O production rates are similar to those for winter and low solar activity, with the exception of a noticeable local maximum near 400 km for energies between 2.4 and 2.6 eV due to reaction (4) (see Figure 8c for a comparison).

Figure 9d shows the normalized hot O kinetic energy source spectra as a function of altitude for summer and high solar activity. The spectrum is dominated by low energies at all altitudes. Examination of Figure 3 reveals that at the lowest energy, hot O is produced dominantly by reaction (24) at the lowest altitudes, and equally by reactions (1) and (24) at higher altitudes. Except at the highest altitudes, reaction (24) produces more hot O than most of the remaining reactions.

Summarizing these results, we can see that at low altitudes the hot O energy source spectra are dominated by the lowest-energy reaction (24) (reaction (1) becomes important at higher altitudes). This is accentuated during high solar activity, where the dominance extends to higher altitudes. During summer and high solar activity, the increased importance of the dissociative recombination of NO^+ (reaction (1)) at high altitudes causes the hot O energy source spectrum to be dominated by the lowest energy at all altitudes. The hot O source spectral characteristics at first glance appear to be dominated by solar cycle variations, with the normalized spectra in Figure 9a resembling those in Figure 9c and those in Figure 9b resembling those in Figure 9d. An exception to this is reaction (9) (energy of 1.65 eV), where relative variations are predominantly seasonal (this occurs because the other dominant sources increase only slightly between winter and summer but increase markedly between low and high solar activity). At high altitudes, the spectral characteristics of the hot O sources are quite variable and depend strongly on season and solar cycle. Overall, the hot O spectrum is cooler during high solar activity, being more so during summer (we again stress that hot O production rates are much greater at high solar activity). Even so, at 0.19 eV the hot O kinetic temperature is approximately 2200 K.

4. Discussion

For reaction (12), which is potentially a large source of hot oxygen at high altitudes, the possibility that N_2^+ is formed in electronically or vibrationally excited states must not be overlooked. Under such conditions, less energy would be directly available for the production of hot O. If vibrational excitation of N_2^+ occurs, the energy of the vibrationally excited N_2^+ would eventually heat the ambient O (unless $N_2^+(A)$ is formed, as discussed in section 2). Therefore the net effect of production of vibrationally excited N_2^+ would be to replace the production of a single hot O atom of energy 0.85 eV by the production of at least two less energetic hot O atoms of combined energy no greater than 0.85 eV. It is possible that similar arguments may apply to other reactions in Table 1 whenever production of molecules and O atoms occurs. However, these considerations lie beyond the scope of this paper. We also note that there is some uncertainty regarding the values of some of the reaction rates, particularly those for reactions (7), (8), and (9).

Our studies of seasonal and solar cycle influences on hot O production were limited to low-latitude conditions. We did examine the latitudinal dependence of hot O production and found some significant variations. For example, while the production rates of hot O due to the dissociative recombination reactions of NO^+ and O_2^+ changed very little with increasing latitude, those due to most of the reactions involving quenching of metastable species and quenching of N_2^* increased several fold at higher latitudes (earlier, we explained these latitudinal variations in production rates of hot O as being a natural consequence of latitudinal variations in both the neutral and ion densities). However, these latter calculations were only performed for summer, moderately high solar activity conditions. These facts suggest that we may have underestimated the importance of some of these new sources of hot O by not examining their seasonal and solar cycle variations at the higher latitude. Nonetheless, the importance of these new sources of hot O, established by *Richards et al.* [1994a] for one very specific set of geophysical conditions, has been generalized here to a wide range of geophysical conditions, while their variability has been quantified.

Finally, we note that in the absence of collisions and for a given suitable trajectory, a hotter oxygen atom will rise to a larger distance above the exobase than will a cooler oxygen atom. Thus we might expect the hotter O atoms to contribute more in the time average toward the hot O geocoronal population. In principal, an oxygen atom having a kinetic energy of 1 eV at the exobase can rise to almost 700 km above the exobase. Using this value with the net exothermicities presented in Table 1 allows determination of the distances above the exobase to which hot O may rise. However, as previously discussed, it is the local production of hot O and not its subsequent transport that we have considered here.

5. Conclusion

We have investigated the importance of 22 new sources of hot oxygen in the thermosphere and compared them with the previously known sources involving dissociative recombination of NO^+ and O_2^+. A detailed study to ascertain the diurnal, latitudinal, seasonal, and solar cycle variations of these sources of hot O has been performed.

We find that quenching of metastable species is a significant but highly variable source of hot oxygen for the exosphere. Under some conditions (e.g., winter, high solar activity), the kinetic energy production rates due to some of these new sources were found to exceed, by a factor of 10, those due to the previously considered O_2^+ and NO^+ dissociative recombination reactions. Here, like *Richards et al.* [1994a], we have found that some of the most significant new sources of hot oxygen are due to reactions involving quenching of $O(^1D)$, $N(^2D)$, $O^+(^2P)$, and vibrationally excited N_2 by atomic oxygen and charge exchange of $N(^2D)$ by O^+ and of $O^+(^2D)$ by N_2.

Although diurnal variations in hot O production rates are large, the relative importance of the various sources appears to change little between day and night. The only exception to this is the source due to reaction (12) (Table 1), which decreases to an insignificant level at night. By contrast, the relative importance of the various hot O sources has a large latitudinal dependence. Although the sources due to the dissociative recombination reactions (1) to (3) change little between the two latitudes considered, those due to the new sources generally increased several fold toward the higher latitude.

Seasonal variations in total hot O production rates appear to be small, although the seasonal variations in the relative importance of some of the individual sources can be large. The largest

variations both in total hot O production and in the relative importance of the individual sources are due to solar cycle variations. Total hot O production is increased by approximately 2 orders of magnitude between solar minimum and solar maximum. However, the hot O is produced substantially cooler at high solar activity compared to that at low solar activity.

Acknowledgments. This work was supported by NSF grants ATM-9224988 and ATM-9018165 and by NASA grant NAGW-996 at the University of Alabama in Huntsville. The authors wish to express their thanks to the reviewers for their helpful comments.
The editor thanks J. L. Fox and another referee for their assistance in evaluating this paper.

References

Abreu, V. J., J.-H. Yee, S. C. Solomon, and A. Dalgarno, The quenching rate of $O(^1D)$ by $O(^3P)$, *Planet. Space Sci., 11*, 1143, 1986.

Chang, T., D. G. Torr, P. G. Richards, and S. C. Solomon, Reevaluation of the $O^+(^2P)$ reaction rate coefficients derived from Atmosphere Explorer C observations, *J. Geophys. Res., 98*, 15,589, 1993.

Cotton, D. M., G. R. Gladstone, and S. Chakrabarti, Sounding rocket observation of a hot oxygen geocorona, *J. Geophys. Res., 98*, 21,651, 1993.

Dalgarno, A., Metastable species in the ionosphere, *Ann. Geophys., 26*, 601, 1970.

Fox, J. L., On the escape of oxygen and hydrogen from Mars, *Geophys. Res. Lett., 20*, 1847, 1993.

Guberman, S. L., and A. Giusti-Suzor, The generation of $O(^1S)$ from the dissociative recombination of O_2^+, *J. Chem. Phys, 95*, 2602, 1991.

Hedin, A. E., MSIS-86 thermosphere model, *J. Geophys. Res., 92*, 4649, 1987.

Hedin, A.E., Hot oxygen geocorona as inferred from neutral exospheric models and mass spectrometer measurements, *J. Geophys. Res., 94*, 5523, 1989.

Ip, W.-H., The fast atomic oxygen corona extent of Mars, *Geophys. Res. Lett.*, 17, 2289, 1990.

Ishimoto, M., M. R. Torr, P. G. Richards, and D. G. Torr, The role of energetic O^+ precipitation in a mid-latitude aurora, *J. Geophys. Res., 91*, 5793, 1986.

Ishimoto, M., G. J. Romick, and C.-I. Meng, Energy distribution of energetic O^+ precipitation into the atmosphere, *J. Geophys. Res., 97*, 8619, 1992.

Knudsen, W. C., Escape of ^{4}He and fast O atoms from Mars and inferences on the ^{4}He mixing ratio, *J. Geophys. Res., 78*, 8049, 1973.

Lie-Svendsen, O., M. H. Rees, and K. Stamnes, Helium escape from the Earth's atmosphere: The charge exchange mechanism revisited, *Planet. Space Sci., 40*, 1639, 1993.

Mahajan, K. K., S. Ghosh, N. K. Sethi, and R. Kohli, Ionospheric evidence of hot oxygen in the upper atmosphere of Venus, *Geophys. Res. Lett., 19*, 1627, 1992.

McElroy, M. B., Mars: An evolving atmosphere, *Science, 175*, 443, 1972.

McNeal, R. J., M. E. Whitson Jr., and G. R. Cook, Temperature dependence of the quenching of vibrationally excited nitrogen by atomic oxygen, *J. Geophys. Res., 79*, 1527, 1974.

Nagy, A. F., and T. E. Cravens, Hot oxygen atoms in the upper atmosphere of Venus and Mars, *Geophys. Res. Lett., 15*, 433, 1988.

Nagy, A. F., T. E. Cravens, J.-H. Yee, and A. I. F. Stewart, Hot oxygen atoms in the upper atmosphere of Venus, *Geophys. Res. Lett., 8*, 629, 1981.

Nagy, A. F., J. Kim, and T. E. Cravens, Hot hydrogen and oxygen atoms in the upper atmospheres of Venus and Mars, *Ann. Geophys., 8*, 251, 1990.

Newton, G. P., J. C. G. Walker, and P. H. E. Meijer, Vibrationally excited nitrogen in stable auroral red arcs and its effect on ionospheric recombination, *J. Geophys. Res., 79*, 3807, 1974.

Omholt, A., The red and near-infra-red auroral spectrum, *J. Atmos. Terr. Phys., 10*, 320, 1957.

Rees, M. H., *Physics and Chemistry of the Upper Atmosphere*, Cambridge University Press, New York, 1989.

Richards, P. G., Thermal electron quenching of $N(^2D)$: Consequences for the ionospheric photoelectron flux and the thermal electron temperature, *Planet. Space Sci., 34*, 689, 1986.

Richards, P. G., M. P. Hickey, and D. G. Torr, New sources for the hot oxygen geocorona, *Geophys. Res. Lett., 21*, 657, 1994a.

Richards, P. G., D. G. Torr, B. W. Reinisch, R. R. Gamache, and P. J. Wilkinson, *F2* peak electron density at Millstone Hill and Hobart: Comparison of theory and measurement at solar maximum, *J. Geophys. Res., 99*, 15,005, 1994b.

Rohrbaugh, R. P., and J. S. Nisbet, Effect of oxygen atoms on neutral density models, *J. Geophys. Res., 78*, 6768, 1973.

Rusch, D. W., D. G. Torr, P. B. Hays, and J. C. G. Walker, The O II(7319-7330 Å) dayglow, *J. Geophys. Res., 82*, 719, 1977.

Shelley, E. G., R. G. Johnson, and R. D. Sharp, Satellite observations of energetic heavy ions during a geomagnetic storm, *J. Geophys. Res., 77*, 6104, 1972.

Shematovich, V. I., D. V. Bisikalo, and J. C. Gerard, Nonthermal nitrogen atoms in the Earth's thermosphere, 1, Kinetics of hot $N(^4S)$, *Geophys. Res. Lett., 18*, 1691, 1991.

Slanger, T. G., and G. Black, Electronic-to-vibrational energy transfer efficiency in the $O(^1D)$-N_2 and $O(^1D)$-CO systems, *J. Chem. Phys., 60*, 468, 1974.

Torr, M. R., and D. G. Torr, The role of metastable species in the thermosphere, *Rev. Geophys., 20*, 91, 1982.

Torr, M. R.., J. C. G. Walker, and D. G. Torr, Escape of fast oxygen from the atmosphere during magnetic storms, *J. Geophys. Res., 79*, 5267, 1974.

Torr, M. R., D. G. Torr, P. G. Richards, and S. P. Yung, Mid- and low-latitude model of thermospheric emissions, 1, $O^+(^2P)$ 7320 Å and N_2 (^2P) 3371 Å, *J. Geophys. Res., 95*, 21,147, 1990.

Torr, M. R., et al., The first negative bands of N_2^+ in the dayglow from the ATLAS 1 shuttle mission, *Geophys. Res., Lett., 20*, 523, 1993.

Yee, J.-H., Non-thermal distribution of $O(^1D)$ atoms in the night-time thermosphere, *Planet. Space Sci., 36*, 89, 1988.

Yee, J-H., and P. B. Hays, The oxygen polar corona, *J. Geophys. Res., 85*, 1795, 1980.

Yee, J.-H., J. W. Meriwether, and P. B. Hays, Detection of a corona of fast oxygen atoms during solar maximum, *J. Geophys. Res., 85*, 3396, 1980.

M. P. Hickey, Center for Space Plasma and Aeronomic Research, OB 300, Huntsville, AL 35899. (e-mail: hickeym@cspar.uah.edu)
P. G. Richards, Computer Science Department, University of Alabama in Huntsville, Huntsville, AL 35899. (e-mail: richards@cs.uah.edu)
D. G. Torr, Physics Department, University of Alabama in Huntsville, Huntsville, AL 35899. (e-mail: torrd@cspar.uah.edu)

(Received May 13, 1994; revised March 13, 1995;
accepted March 14, 1995.)